Human in vivo neuroimaging to detect reprogramming of the cerebral immune response following repeated systemic inflammation

Peters van Ton, Annemieke M; Leijte, Guus P; Franssen, Gerben M; Bruse, Niklas; Booij, Jan; Doorduin, Janine; Rijpkema, Mark; Kox, Matthijs; Abdo, Wilson F; Pickkers, Peter

Published in:
Brain, Behavior, and Immunity

DOI:
10.1016/j.bbi.2021.04.004

Publication date:
2021

Brain, Behavior, and Immunity 95 (2021) 321–329

Contents lists available at ScienceDirect

Brain Behavior and Immunity

journal homepage: www.elsevier.com/locate/ybrbi

Human *in vivo* neuroimaging to detect reprogramming of the cerebral immune response following repeated systemic inflammation

Annemieke M. Peters van Ton [a,b], Guus P. Leijte [a,b], Gerben M. Franssen [c], Niklas Bruse [a,b], Jan Booij [c,d], Janine Doorduin [e], Mark Rijpkema [c], Matthijs Kox [a,b,1], Wilson F. Abdo [a,b,1,*], Peter Pickkers [a,b,1]

[a] Radboud University Medical Center, Radboud Institute for Molecular Life Sciences, Department of Intensive Care Medicine, Nijmegen, the Netherlands
[b] Radboud University Medical Center, Radboud Center for Infectious Diseases, Nijmegen, the Netherlands
[c] Radboud University Medical Center, Radboud Institute for Health Sciences, Department of Medical Imaging, Nijmegen, the Netherlands
[d] Amsterdam University Medical Centers, Location Academic Medical Center, University of Amsterdam, Department of Radiology & Nuclear Medicine, Amsterdam, the Netherlands
[e] University of Groningen, University Medical Center Groningen, Department of Nuclear Medicine and Molecular Imaging, Groningen, the Netherlands

ARTICLE INFO

Keywords:
Neuroinflammation
Innate immunity
Lipopolysaccharide
TSPO neuroimaging
Cerebral immunotolerance

ABSTRACT

Despite increasing evidence that immune training within the brain may affect the clinical course of neuropsychiatric diseases, data on cerebral immune tolerance are scarce. This study in healthy volunteers examined the trajectory of the immune response systemically and within the brain following repeated lipopolysaccharide (LPS) challenges. Five young males underwent experimental human endotoxemia (intravenous administration of 2 ng/kg LPS) twice with a 7-day interval. The systemic immune response was assessed by measuring plasma cytokine levels. Four positron emission tomography (PET) examinations, using the translocator protein (TSPO) ligand ^{18}F-DPA-714, were performed in each participant, to assess brain immune cell activation prior to and 5 hours after both LPS challenges. The first LPS challenge caused a profound systemic inflammatory response and resulted in a 53% [95%CI 36–71%] increase in global cerebral ^{18}F-DPA-714 binding ($p < 0.0001$). Six days after the first challenge, ^{18}F-DPA-714 binding had returned to baseline levels ($p = 0.399$). While the second LPS challenge resulted in a less pronounced systemic inflammatory response (i.e. 77 ± 14% decrease in IL-6 compared to the first challenge), cerebral inflammation was not attenuated, but decreased below baseline, illustrated by a diffuse reduction of cerebral ^{18}F-DPA-714 binding (-38% [95%CI -47 to -28%], $p < 0.0001$). Our findings constitute evidence for *in vivo* immunological reprogramming in the brain following a second inflammatory insult in healthy volunteers, which could represent a neuroprotective mechanism. These results pave the way for further studies on immunotolerance in the brain in patients with systemic inflammation-induced cerebral dysfunction.

1. Introduction

The discovery of innate immune cell memory shifted our understanding of innate immunity profoundly (Kurtz, 2005; Medzhitov and Janeway, 2000; Netea et al., 2011). On one end of the spectrum, innate immune cells exposed to microbial components exhibit an enhanced pro-inflammatory phenotype following subsequent restimulation with unrelated stimuli. This phenomenon was coined 'trained immunity' (Netea et al., 2011). On the other end of the spectrum, an initial challenge of innate immune cells with potent immunostimulants such as bacterial lipopolysaccharide (LPS) results in a severely blunted inflammatory response after restimulation with the same or a different compound. This response is known as 'immunotolerance' or 'immunoparalysis' (Netea et al., 2016). Both trained immunity and immunotolerance may exhibit beneficial as well as detrimental consequences for the host.

In the central nervous system (CNS), neuroinflammation has been shown to play an intricate role in the pathogenesis of neuropsychiatric

* Corresponding author at: Department of Intensive Care Medicine, IP 707, Radboud University Medical Center, P.O. Box 9101, 6500 HB Nijmegen, The Netherlands.
E-mail address: f.abdo@radboudumc.nl (W.F. Abdo).
[1] Shared last authorship.

https://doi.org/10.1016/j.bbi.2021.04.004
Received 17 December 2020; Received in revised form 17 March 2021; Accepted 7 April 2021
Available online 9 April 2021

disorders such as major depression, psychotic disorders, Alzheimer's disease (AD), Parkinson's disease, and amyotrophic lateral sclerosis (Brites and Fernandes, 2015; Heneka et al., 2015; Mondelli et al., 2017; Philips and Robberecht, 2011; Vivekanantham et al., 2015). Up to now, innate immune memory of the brain has almost solely been studied within the trained immunity field. Several studies showed that systemic inflammation may induce an exaggerated pro-inflammatory response in the brain when CNS innate immune cells were previously chronically activated (Combrinck et al., 2002; Cunningham et al., 2009, 2005; Godbout et al., 2005; Hughes et al., 2010; Lopez-Rodriguez et al., 2018; Palin et al., 2008; Raj et al., 2014; Ramaglia et al., 2012; Yin et al., 2017). This hyperreactive cell phenotype is referred to as priming of CNS immune cells, in which pro-inflammatory cytokines produced by glial cells promote sustained tissue inflammation and a neurotoxic microenvironment (Kettenmann et al., 2011), ultimately resulting in exacerbation of brain pathology (Perry et al., 2007; Wendeln et al., 2018).

In contrast, the concept of immunotolerance of the brain has been sparsely investigated. *In vitro* and animal experiments have shown that LPS-preconditioned microglia acquire an immune-suppressed phenotype (Schaafsma et al., 2015). In addition, single peripheral administration of LPS in mice induced immune training, whereas repeated challenges induced immune tolerance (Wendeln et al., 2018). Interestingly, immunotolerance alleviated cerebral β-amyloidosis load in a murine AD model and led to less severe stroke pathology (Wendeln et al., 2018). These animal data combined with observational data in humans (Ehlenbach et al., 2010; Honarmand et al., 2020; Moller et al., 1998; Monk et al., 2008; Pandharipande et al., 2013; Shah et al., 2013; Wolters et al., 2013) suggest that cerebral innate immune memory plays an important role in neurodegeneration. However, *in vivo* data on the trajectory of innate immune memory within the human brain is non-existing.

Experimental human endotoxemia, in which LPS is intravenously administered to healthy volunteers, induces a standardized, reproducible, and safe, transient systemic inflammatory response (van Lier et al., 2019). LPS administration also results in the development of endotoxin tolerance, which is exemplified by a profoundly attenuated immune response after a second challenge with LPS (Leentjens et al., 2012; Leijte et al., 2018; van Lier et al., 2019). This refractory state of the immune system captures many hallmarks of the immunotolerant state observed after sepsis or major surgery (Leentjens et al., 2012; Leijte et al., 2018; van Lier et al., 2019). Previous work has shown that cerebral positron emission tomography (PET) imaging using radiotracers targeting the mitochondrial translocator protein (TSPO) can be employed to measure microglial and astrocytic activation *in vivo* during systemic inflammation (Forsberg et al., 2017; Nettis et al., 2020; Sandiego et al., 2015; Woodcock et al., 2020). TSPO binding is minimal in healthy brains, but markedly increased after activation of microglia and astrocytes (Lavisse et al., 2012; Rupprecht et al., 2010).

In the present study, we employed this imaging paradigm combined with repeated endotoxemia to study the *in vivo* immune response trajectories within the systemic and brain compartment.

2. Materials and methods

2.1. Subjects and ethical approval

Six healthy male volunteers (aged 18–35 years) were recruited. Exclusion criteria included smoking, use of medication, signs of acute illness in the three weeks prior to start of the study, previous participation in experimental human endotoxemia, previous neurotrauma, past psychiatric or substance dependence diagnosis, and contra-indications to undergo a MRI-scan. Written informed consent was obtained, and medical history, physical examination, laboratory tests, and a 12-leads electrocardiogram did not reveal abnormalities. Prior to inclusion, subjects were genotyped for the rs6971 polymorphism on the TSPO gene to exclude low-affinity TSPO binders (homozygous T/T). For this, DNA was extracted from blood samples, and the rs6971 polymorphism was genotyped using Taqman analysis on a 7500 Fast Real-Time PCR System (ThermoFisher Scientific, Waltham, USA). Four participants were high-affinity binders, and two were mixed-affinity binders. Due to the small sample size and the within-subject design, these were analyzed as one group, however, sensitivity analysis did not reveal different outcomes if TSPO genotype was incorporated in the analyses. This study was part of a human endotoxemia project that was approved by the Medical Research Ethics Committee (MREC) region Arnhem-Nijmegen (NL61136.091.17 and 2017-3337). The study procedures were performed in accordance with the declaration of Helsinki.

2.2. Study design

In this study, subjects received two subsequent LPS challenges, with an interval of 7 days. Subjects underwent ^{18}F-DPA-714 dynamic PET/CT imaging of the brain to study the neuroinflammatory response following the LPS challenges at four timepoints: before the first LPS challenge (first baseline), 5 hours after the first challenge, 6 days later (second baseline) and 5 hours after the second challenge at day 7. Furthermore, a structural T1-weighted MRI of the brain was obtained on a 3 T TIM TRIO scanner (Siemens, Erlangen, Germany) at baseline for anatomical co-registration of the PET/CT images. Blood was collected before and at numerous timepoints after the LPS challenges as well as during the PET/CT scans to characterize the systemic immune response and for pharmacokinetic analysis of the PET-data, respectively. This study design is illustrated in Fig. 1A.

2.3. Experimental human endotoxemia

Subjects were admitted twice to the intensive care research unit of the Radboud university medical center in Nijmegen, The Netherlands, to receive both LPS challenges. All subjects underwent the same procedures on both hospitalization days which were 7 days apart. One day prior to both admissions, subjects needed to refrain from alcohol and caffeine, and no food or drinks were allowed from 10 hours before start of the challenge days. After admission, an intravenous cannula was inserted in the antebrachial vein to administrate fluids and LPS. A radial artery catheter was placed to withdraw blood and monitor blood pressure continuously. One hour before the challenge, 1.5 L prehydration fluid (2.5% Glucose/0.45% NaCl) was administered. Subsequently, a bolus of 2 ng/kg LPS (*E. coli type O113, Lot no. 94332B1;* List Biological Laboratories, Campbell, USA) was administered intravenously and similar hydration fluid was continued at an infusion rate of 150 mL/h for 8 hours. Heart rate was monitored using a 4-lead electrocardiogram (M50 Monitor, Philips, Eindhoven, The Netherlands) and intra-arterial blood pressure was measured with a pressure transducer (Edward Lifesciences, Irvine, USA). Every 30 minutes, we measured core temperature with a tympanic thermometer (FirstTemp Genius 2, Covidien, Dublin, Ireland) and LPS-induced symptoms (headache, nausea, cold shivers, muscle- and back pain) were scored using a numeric six-point scale (0 = no symptoms, 5 = worst symptoms experienced ever). The sum of these scores in addition of 3 points in case of vomiting, resulted in a total symptom score ranging from 0 to 28. Blood was withdrawn before prehydration (T = -60 minutes), just before LPS administration (T = 0 minutes), and respectively 60, 90, 120, 180, 240, 360 and 480 minutes after the LPS bolus. Plasma cytokine concentrations (tumour necrosis factor-alpha (TNF-α), interleukin (IL)-6, IL-8, IL-10, macrophage inflammatory protein (MIP)-1α, MIP-1β, monocyte chemoattractant protein (MCP)-1 and IL-1RA (receptor antagonist)) were determined batchwise using a simultaneous luminex assay (Milliplex, Millipore, Billerica, USA).

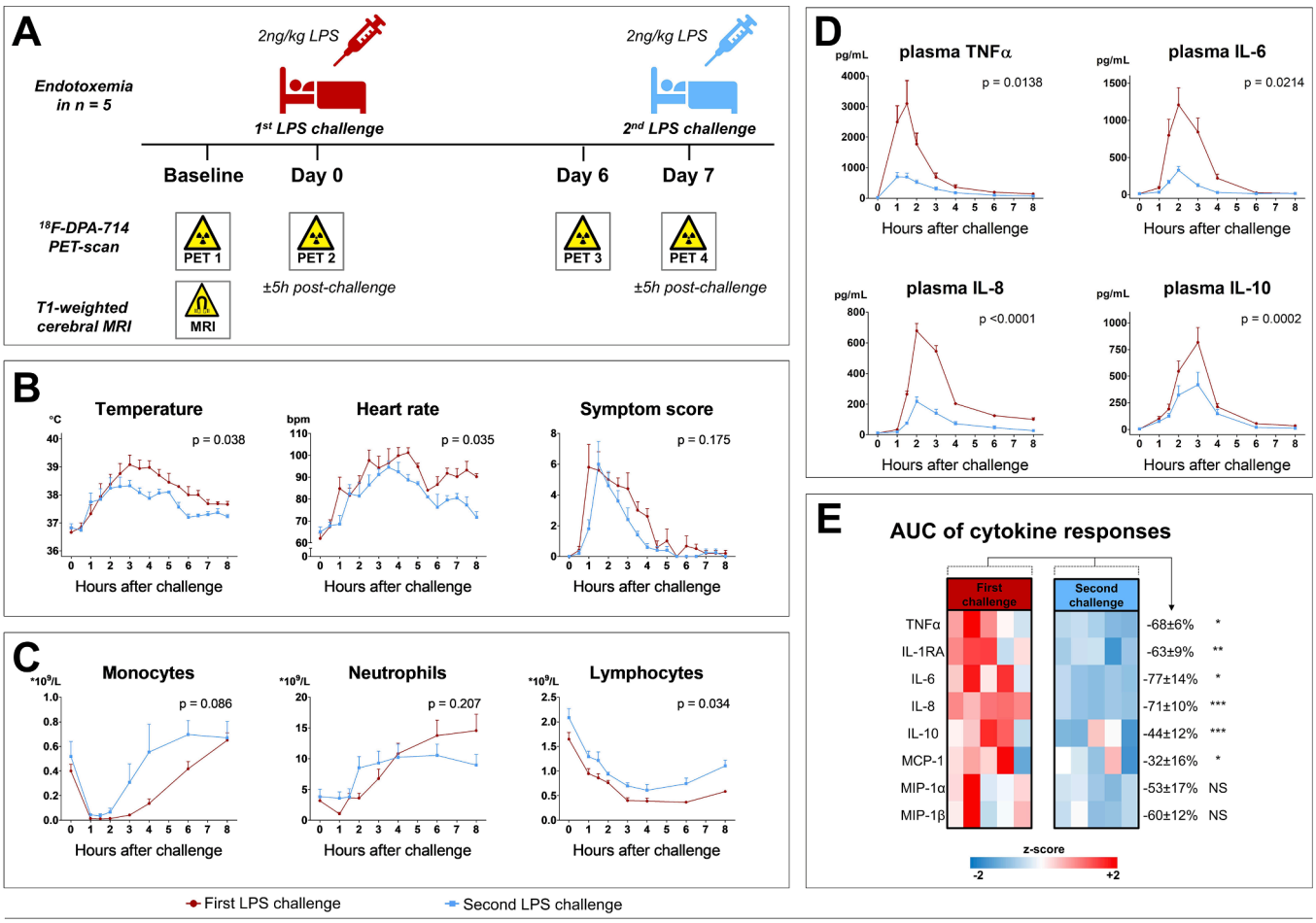

Fig. 1. Study design (**A**) and systemic inflammatory responses (**B-E**): Five healthy volunteers underwent repeated intravenous LPS challenges (2 ng/kg E. coli-derived lipopolysaccharide (LPS) with an interval of 7 days. TSPO brain PET imaging with the radiotracer ^{18}F-DPA-714 was performed at 4 timepoints: prior to and approximately 5 hours after each LPS challenge. At baseline a T1-weighted structural cerebral MRI was performed for anatomical coregistration (**A**). The systemic inflammatory response following LPS challenges is reflected by changes in (**B**) vital parameters (mean + SEM), (**C**) leukocyte subset counts (mean + SEM), (**D**) plasma cytokine concentrations (mean + SEM), and (**E**) area under the cytokine (AUC) response curve. Responses after the first LPS challenge in B, C, and D are depicted in red circles, the blue squares depict responses after the second LPS challenge. Abbreviations: ^{18}F-DPA-714: 18-fluoride labelled N,N-diethyl-2-[4-(3-fluoroethoxy) phenyl]-5,7-dimethylpyrazolo[1,5-a]pyrimidine-3-acetamide; bpm: beats per minute; TNFα: tumour necrosis factor alpha; IL: interleukin; MCP-1: monocyte chemoattractant protein 1; MIP: macrophage inflammatory protein; IL-1RA: interleukin-1 receptor antagonist; p-values in B-D were tested with repeated measures two-way ANOVA. * $p < 0.05$; ** $p < 0.01$, *** $p < 0.001$ and NS = not significant in E, according to paired t-tests on AUC. (For interpretation of the references to colour in this figure legend, the reader is referred to the web version of this article.)

2.4. TSPO neuroimaging – PET acquisition and image reconstruction

Each subject participated in four ^{18}F-DPA-714 PET scan sessions prior to and approximately five hours after each LPS challenge. This timing was chosen since we expected increased TSPO expression at this moment, and to reduce the risk on movement-induced artefacts due to LPS-induced symptoms. The interval between LPS administration and the post-LPS scan varied slightly between subjects (5.00 h – 5.45 h) but within-subject the interval was exactly the same for both post-LPS scans. ^{18}F-DPA-714 was synthesized at the Radionuclide Centre of VUmc, Amsterdam, The Netherlands, as previously described (Golla et al., 2015). The specific activity at the end of synthesis was 40.3 ± 11.0 GBq/μmol and the average radiochemical purity was greater than 99%. Three batches did not pass quality control and since these concerned post-LPS scans, and LPS had to be administered to the volunteers before the radiotracer synthesis was concluded, we could not reschedule these missed scans. ^{18}F-DPA-714 (123 ± 5 MBq) was injected intravenously as a bolus over 40 seconds by a computer-controlled pump (OptiVantage® Multi-use, Guerbet, Paris, FR). Sixty minutes dynamic PET scans were acquired on a Biograph 40mCT scanner (Siemens Medical Solutions, Erlangen, Germany) of the brain region (15 cm field of view (FOV)), starting at time of injection. Before each radiotracer administration, an ultra-low dose brain CT-scan (80 kV, 30 mA) was acquired for attenuation correction of the PET emission data. Dynamic list-mode scan data were reconstructed into 32 frames (18 × 10 s, 4 × 30 s, 5 × 1 min, and 5 × 10 min) using the Ordered Subset Expectation Maximization (21 subsets and 3 iterations) with inclusion of time of flight, attenuation correction, and in-plane gaussian post smoothing (Full Width at Half Maximum kernel of 3 mm).

2.5. TSPO neuroimaging – Arterial input function and metabolite correction

Metabolite-corrected arterial input functions were collected and used for pharmacokinetic modelling to estimate ^{18}F-DPA-714 binding. Arterial blood samples were taken manually immediately before ^{18}F-DPA-714 injection and during the scan ~ every 2 seconds for the first 2 minutes, and at 2.5, 3.0, 4.0, 6.0, 8.0, 10.0, 20.0, 30.0, 40.0, 50.0 and 59.5 minutes after injection. Radioactivity in a sub-selection of whole blood samples was measured using an automated gamma-counter (Wizard^2 2480, PerkinElmer, USA). All blood samples were centrifuged and the amount of radioactivity in plasma was additionally

measured. Then the ratio between whole blood and plasma was calculated to generate a population based whole blood/plasma ratio. This ratio was applied to the individual plasma curves to generate a whole blood curve. In three samples per subject, obtained at 3, 10, and 30 minutes after tracer injection, during post-LPS scans from two participants, the ^{18}F-DPA-714 parent fraction curve was determined, using solid phase extraction as described previously (Peyronneau et al., 2013). The metabolite-corrected arterial input function was calculated as the product of the plasma time-activity curve and parent fraction curve. The arterial input function in two scans had technical failures and were excluded from the analysis.

2.6. TSPO neuroimaging – Image processing and analysis

PET data analysis was performed using PMOD 4.0 software (PMOD Technologies LLC, Zürich, Switzerland). First, the MR images were segmented using the 6 Probability Maps and the PET images were matched to the MR images. Then, the Hammers Atlas was spatially normalized to the PET images. Volume-of-interests (VOI) of individual brain regions were automatically derived to obtain time-activity curves (TACs, in kBq/ml). These included the frontal, parietal, temporal and occipital lobes, thalamus, hippocampus, amygdala, brainstem, cerebellum and whole brain. The metabolite-corrected arterial plasma activity curve was used as input function to estimate the binding potential (BP_{ND}, k_3/k_4) in each VOI. BP_{ND} is the product of receptor density and affinity of ligand binding and dependent on the fraction of non-displaceable binding in the tissue (Innis et al., 2007; Mintun et al., 1984). BP_{ND} may be directly related to TSPO receptor expression and thus glial activation. In this study, the 2TCM K_1/k_2 with K_1/k_2 constrained for gray matter VOIs, showed more reliable (smaller SE) values for BP_{ND}, compared to the 2TCM, 2TCM K_1/k_2 and to the 2TCM with vascular trapping (2TCM-1 K) (Rizzo et al., 2014), and was therefore reported. The change in BP_{ND} (%ΔBP_{ND}) across brain regions from the first baseline (PET 1) was computed as (BP_{ND} PET2/3/4 – BP_{ND} PET1) / BP_{ND} PET 1 *100%. For visualization of global PET tracer uptake, standardized uptake value (SUV) images were calculated in PMOD with averaged time frames.

2.7. TSPO mRNA expression and ^{18}F-DPA-714 binding on peripheral blood cells

The methodology of assessing TSPO mRNA expression on peripheral blood cells and the *in vitro* ^{18}*F-DPA-714* binding assay is described in the Supplementary Information.

2.8. Statistical analysis

Statistical analyses were performed with R software packages, version 3.6.2 (http://www.R-project.org) and GraphPad version 6.0 (Sandiego, USA). Results are reported as mean + SEM or median with interquartile range (IQR), depending on the distribution. Area under the curves (AUC) were calculated and systemic responses following the first and second LPS challenge were compared with paired t-tests. To examine differences in ^{18}F-DPA-714 scan parameters between baseline and follow-up scans, log-transformed BP_{ND} were analyzed using a linear mixed model with time of the PET-scan as within-subjects fixed effect, and subject ID and brain region as random effects. In addition we analyzed the data with time and cortical region as fixed effects to assess differences in the neuroinflammatory response in cortical and other brain regions. Pearson correlations were performed between the AUC of cytokine and leukocyte responses, and vital signs, and the percentage delta in frontal BP_{ND} (%ΔBP_{ND}) after both LPS challenges, to assess whether the systemic inflammatory response correlates with the immune response of the brain.

3. Results

Fig. 1A illustrates the study procedures. Six healthy male volunteers aged 24 ± 4 years, with a body mass index (BMI) of 24.7 ± 1.5 were included. From one subject, the baseline PET results deviated more than 2 SD from the mean and was regarded an outlier. Since the second baseline of this subject was missing due to issues with PET tracer synthesis, no baseline measurement was available and therefore this subject was excluded from the analysis. eTable 1 illustrates the homogeneity of the cohort.

3.1. Characterization of the systemic immune response after repeated endotoxemia

The first LPS challenge induced a profound systemic inflammatory response, characterized by fever, flu-like symptoms (including headache and shivering), and haemodynamic changes (Fig. 1B). Kinetics in leukocyte differentiation are illustrated in Fig. 1C. Plasma concentrations of both pro-inflammatory and anti-inflammatory cytokines increased substantially following the first LPS challenge and most returned to baseline levels within 8 hours (Fig. 1D and eFigure 1). Seven days later, all inflammatory parameters had returned to baseline values. The second LPS challenge resulted in an attenuated inflammatory response (Fig. 1B-D and eFigure 1), with an approximately 60% less pronounced cytokine response compared to the first (Fig. 1E), illustrative of systemic immunotolerance *in vivo*.

3.2. The first but not the second LPS challenge significantly increases glial activity

There were no significant differences before or after LPS challenges with regard to injected radiotracer volumes (8.0 ± 0.1 mL vs. 8.0 ± 0.1 mL, respectively, $p = 0.49$) or dose of radioactivity (122.8 ± 4.4 MBq vs. 123.1 ± 6.2 MBq, respectively, $p = 0.79$). Three post-LPS scans were cancelled due to radiotracer synthesis batches not passing quality control and two scans (one pre-LPS and one post-LPS) had to be excluded from the analysis due to technical failures. Therefore fifteen scans were included in the final analysis ($n = 9$ and $n = 6$ PET scans prior to and after LPS challenges, respectively). Sensitivity analyses between subjects with complete follow-up and subjects with missing scans did not reveal case-mix differences.

Fig. 2 shows diffuse uptake of ^{18}F-DPA-714 throughout the brain. The ^{18}F-DPA-714 binding potential (BP_{ND}), which is related to TSPO receptor density and thus a marker for glial activity, was measured in regions of interest for baseline and LPS challenge scans. Table 1 presents the trajectory of regional BP_{ND} values. The first LPS administration significantly increased whole brain BP_{ND} (+53% [95%CI 36–71%], $p < 0.0001$). This increase was most pronounced in cortical brain regions (+89% [95%CI 33–167%], $p = 0.0002$), and less in subcortical regions (+28% [95%CI 12–48%], $p = 0.0005$), which is illustrated in Fig. 3. Importantly, analysis of the kinetic parameter representing influx of the radiotracer between the blood and brain compartment did not suggest a change in blood brain barrier (BBB) permeability or blood flow after the LPS challenges. Six days after the first LPS challenge, BP_{ND} had returned to levels similar to those observed before the first challenge (Table 1 and Fig. 3). Although the second endotoxemia at day 7 induced a less pronounced systemic inflammatory response compared to the first, reflecting systemic immunotolerance, clear increases in all systemic inflammatory parameters were still present as described before. In contrast to these systemic findings, whole brain BP_{ND} was not attenuated, but significantly decreased below baseline levels following the second challenge (-38% [95%CI -47 to -28%], $p < 0.0001$, Table 1 and Fig. 3). This decrease was similar across all studied brain regions (Table 1 and Fig. 3).

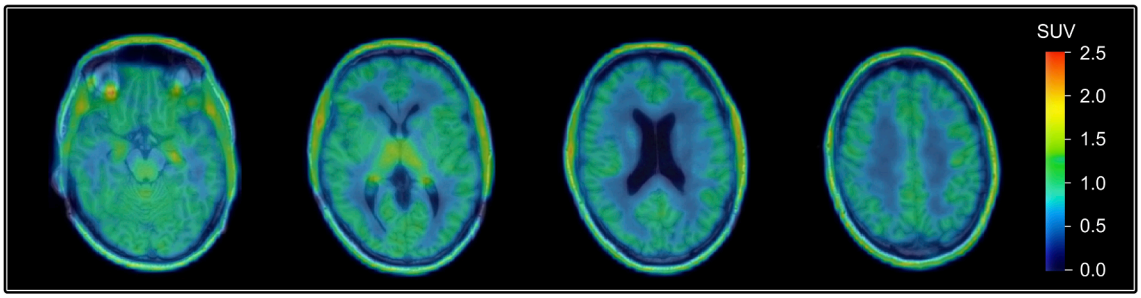

Fig. 2. Transverse slides from the first baseline scan showing diffuse uptake of ^{18}F-DPA-714 throughout the brain. *Merged PET and T1 MR images from a representative subject SUV: standardized uptake value averaged for the final 30 minutes.*

Table 1
^{18}F-DPA-714 regional BP_{ND} values (median [IQR]) and percentage differences relative to each baseline (median [IQR]).

Brain region	1st Baseline $n = 5$	5 h post-LPS challenge 1 $n = 4$	%Δ BP^1_{ND}	2nd Baseline $n = 4$	5 h post LPS challenge 2 $n = 2$	%Δ BP^2_{ND}
Frontal	0.72[0.65–1.04]	1.53[1.26–1.76]	*115[83–151]*	0.75[0.62–0.92]	0.48[0.42–0.55]	*-45[-48 to -43]*
Parietal	0.74[0.67–0.80]	1.50[1.29–2.11]	*117[80–161]*	0.71[0.65–0.88]	0.44[0.35–0.53]	*-48[-53 to -42]*
Temporal	0.76[0.66–0.84]	1.53[0.70–2.00]	*119[-8 – 151]*	0.77[0.60–0.92]	0.51[0.38–0.63]	*-44[-55 to -33]*
Occipital	0.84[0.74–0.93]	1.69[1.11–2.06]	*110[39–137]*	0.78[0.60–0.97]	0.53[0.44–0.62]	*-43[-48 to -38]*
Hippocampus	0.93[0.76–1.16]	1.42[0.74–1.83]	*50[-10–69]*	1.02[0.68–1.44]	0.57[0.50–0.65]	*-51[-68 to -33]*
Amygdala	0.84[0.78–1.14]	1.61[0.90–1.83]	*55[10–104]*	1.01[0.85–1.29]	0.55[0.52–0.57]	*-54[-58 to -50]*
Thalamus	0.97[0.93–1.39]	1.38[1.33–1.99]	*34[32–46]*	1.20[0.80–1.45]	0.90[0.81–0.98]	*-37[-40 to -34]*
Brain stem	1.44[1.24–1.55]	1.85[0.89–2.33]	*24[–33–50]*	1.41[1.24–1.81]	1.12[1.06–1.17]	*-30[-39 to -21]*
Cerebellum	0.77[0.72–0.90]	1.63[0.70–1.86]	*84[−13–134]*	0.90[0.57–1.10]	0.68[0.66–0.70]	*-37[-41 to -34]*

%ΔBP_{nd}: percentage change in binding potential (BP_{ND}) from baseline ([1]:post-LPS challenge 1 vs. 1st baseline and [2]: post-LPS challenge 2 vs. 2nd baseline) for subjects with paired measurements.

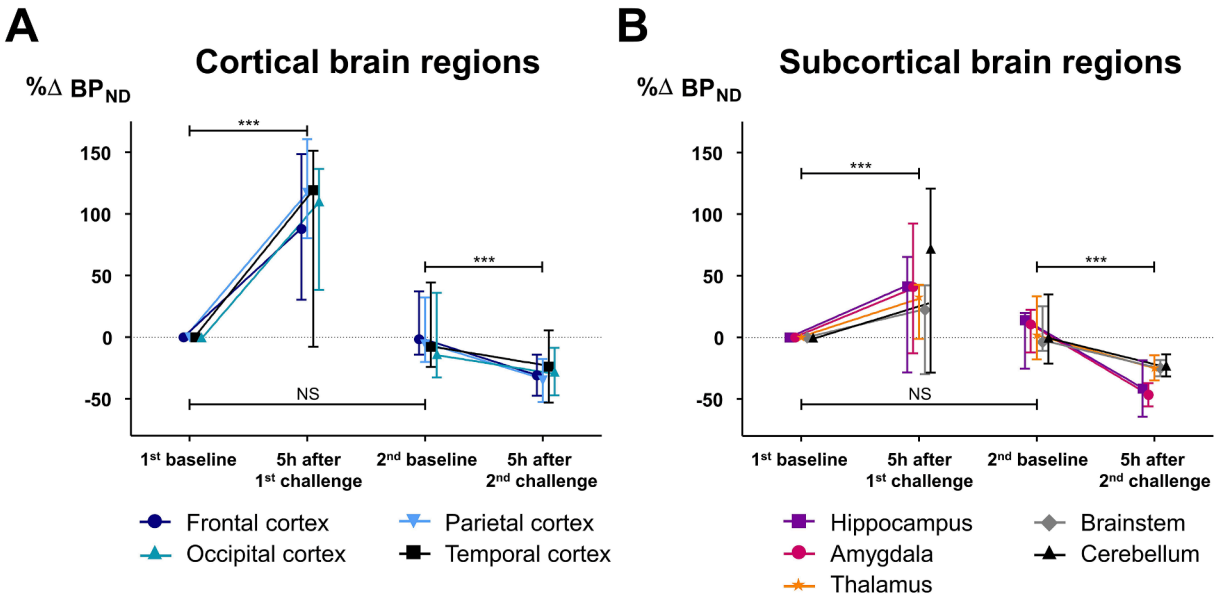

Fig. 3. The percentage change in ^{18}F-DPA-714 binding potential from baseline in cortical (**A**) and subcortical brain regions (**B**). *%Δ BP_{ND}: percentage change in ^{18}F-DPA-714 binding potential relative to the first baseline, median [IQR]. *** $p < 0.001$; NS: not significant according to linear mixed modelling of* log*-transformed BP_{ND} results, with time and region as fixed factors and subject ID as random effect.*

3.3. Correlations between systemic and cerebral immune responses

To assess whether systemic inflammatory response parameters were related to the brain immune response, we performed correlation analyses between the area under the curve (AUC) cytokine and leukocyte responses, vital parameters, and the percentage change in frontal BP_{ND} (%ΔBP_{ND}) after both LPS challenges. Fig. 4 shows strong positive correlations between the endotoxemia-induced increase in heart rate ($R^2 = 0.80$, $p = 0.017$) and body temperature ($R^2 = 0.73$, $p = 0.031$), as well as the pro-inflammatory cytokines IL-6 ($R^2 = 0.79$, $p = 0.017$) and IL-8 ($R^2 = 0.79$, $p = 0.018$) with %ΔBP_{ND}.

3.4. TSPO mRNA expression on peripheral monocytes

Single-cell RNA sequencing analysis revealed that approximately 55% of circulating classical monocytes do not express TSPO mRNA, and this fraction does not change following a LPS challenge. In the subset of monocytes expressing TSPO mRNA, slightly but significantly increased

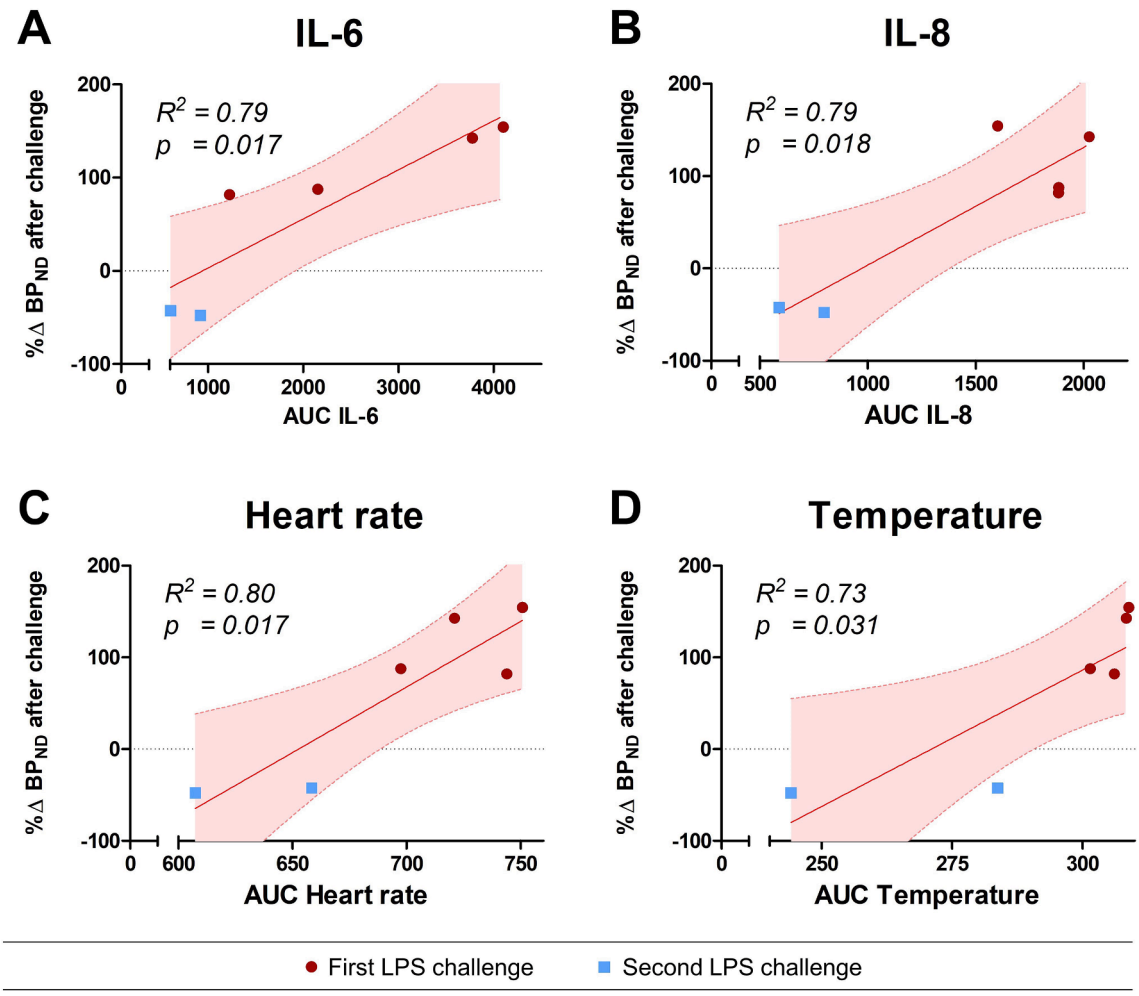

Fig. 4. Pearson correlation between systemic inflammatory responses and the percentage change in frontal BP_{ND} following LPS challenges. Systemic inflammatory response reflected by the area under the curves (AUC) of the pro-inflammatory cytokines interleukin (IL)-6 (**A**) and IL-8 (**B**), heart rate (**C**) and temperature (**D**). Frontal BP_{ND} (%Δ BP_{ND}) was chosen as example for cortical TSPO binding. Regression line with 95% confidence intervals. The red circles indicate the responses after the first LPS challenge and the blue squares indicate the responses after the second challenge. (For interpretation of the references to colour in this figure legend, the reader is referred to the web version of this article.)

expression was observed 4 hours after the first LPS challenge, which reverted to baseline after 7 days (eFigure 2).

3.5. ^{18}F-DPA-714 binding to peripheral blood cells

In addition to TSPO mRNA levels in peripheral monocytes, we evaluated whether this resulted in functional changes of ^{18}F-DPA-714 binding of peripheral blood cells, to allow for comparison with the observed changes in binding potential of cerebral immune cells. To this end, we performed an *in vitro* binding assay using whole blood obtained before and 4 hours after LPS administration. eFigure 3 shows a significant 70 ± 7% decrease of plasma/pellet ratio 4 hours after LPS administration ($p = 0.012$), indicating increased ^{18}F-DPA-714 binding to peripheral blood cells during systemic inflammation.

4. Discussion

In the current study, we demonstrate that an initial LPS challenge induced robust glial activation, reflected by diffusely increased TSPO binding in the brain, in particular in cortical brain regions. This response was relatively short-lived, as TSPO binding returned to baseline 6 days later. Following the second LPS challenge on day 7, we observed not increased but rather reduced cerebral TSPO binding, which suggests reprogramming of the brain immune response following LPS-induced systemic inflammation in healthy young male volunteers. Our data also revealed that cerebral and systemic immune responses are strongly correlated. These are important findings, as they indicate the development of cerebral immunotolerance in humans *in vivo* as a possible brain-protective mechanism.

The Toll-like receptor (TLR) 4 agonist LPS activates innate immune cells to release pro-inflammatory cytokines, which, among others, results in the recruitment of other immune cells. LPS administration has clear effects on brain functioning as reflected clinically by sickness behaviour, headache, nausea and hyperthermia (Schedlowski et al., 2014). The human endotoxemia model enabled us to study the cerebral immune response following a standardized systemic inflammatory stimulus. The profound increase in glial activity observed following the first LPS challenge is in line with previous work (Sandiego et al., 2015; Woodcock et al., 2020), but our study significantly extends these findings. First, our data indicate that the pro-inflammatory state of glial cells following a LPS challenge is relatively short-lived, confirming that the experimental human endotoxemia model can be safely used to study neuroinflammation in healthy volunteers. Second, following the second LPS challenge, cerebral TSPO binding potential was decreased, suggestive of reprogramming of the cerebral immune response. One could argue that this was due to a blunted systemic immune response, which in turn may be less sufficient to activate microglia and astrocytes. However, the second LPS challenge still elicited a clear systemic

inflammatory response, including clinical features such as tachycardia and hyperthermia, as well as significant increases in plasma cytokine levels, albeit less pronounced compared to the first challenge. A previous study also demonstrated increased TSPO binding after a single LPS administration, using a 50% lower dose than we used (Sandiego et al., 2015). If the brain were to follow the systemic compartment, we would have expected an increase in TSPO binding following both LPS challenges with a milder increase during the second endotoxemia, rather than the observed decrease following the second LPS challenge.

Thus far, research on immune memory within the neuroinflammation field mainly focused on trained immunity, while cerebral immunotolerance is less well studied. Recent studies demonstrated that increased TSPO binding is specific for pro-inflammatory activated glial cells in the brain in response to inflammatory stimuli (Beckers et al., 2017; Pannell et al., 2020). Since TSPO binding actively decreased during the second endotoxemia, our findings indicate that our healthy volunteers developed reprogramming towards less cerebral pro-inflammation, which may indicate cerebral immunotolerance. In view of the associations between neuroinflammation and neurodegenerative diseases (Cunningham et al., 2009; Heneka et al., 2015; Perry et al., 2007; Vivekanantham et al., 2015), this immunotolerant phenotype within the brain might serve as a neuroprotective response to reduce inflammation-associated neurotoxicity (Boche et al., 2006; Thackray et al., 2004). Since peripheral immunotolerance is defined as a less pronounced, but still present, pro-inflammatory response upon subsequent stimuli, the decrease in TSPO binding below baseline may not reflect a tolerant state but rather a counterregulatory response. A decrease in TSPO binding from baseline suggests a less pro-inflammatory phenotype, possibly mediated by a more anti-inflammatory environment in the brain. This remains speculation as an *in vivo* biomarker for anti-inflammatory microglial activity is currently not available. Our exploratory data justify future studies to confirm reprogramming of the cerebral immune response and to explore to what extent cerebral immunotolerance leads to an anti-inflammatory, neuroprotective phenotype in the brain.

In a first, and to date only, clinical TSPO neuroimaging study in patients undergoing surgery, a global decrease of TSPO binding was found 3–4 days after prostatectomy (Forsberg et al., 2017). Interestingly, animal disease models with repeated LPS and concomitant cerebral immunotolerance demonstrated decreased β-amyloid plaque load and modulated stroke pathology (Wendeln et al., 2018). Currently, the effects of cerebral immunotolerance on tau phosphorylation, an important inductor of neurodegeneration, are unknown, and this forms an interesting aim for future studies. A post-mortem study in Alzheimer patients demonstrated an immunosuppressed microglial phenotype in patients who died during infections relative to patients who died without infection (Rakic et al., 2018), indicating the modification of neuroinflammatory processes by systemic inflammation. Cerebral immunotolerance could be a beneficial response to prevent neuroaxonal damage due to exaggerated neuroinflammation. One could argue that in those patients with brain dysfunction, e.g. delirium or long-term cognitive decline following a systemic inflammatory insult, the balance between pro-and anti-inflammatory responses is skewed to excessive pro-inflammation. A brain-specific intervention aimed at polarization towards a more immunosuppressive state (Rinaldi et al., 2016; Song and Suk, 2017) could therefore have therapeutic potential in certain patients. Future studies, including markers for cognitive and mental functioning, are however warranted to validate these hypotheses.

The present study is the first to study neuroinflammatory responses, using longitudinal PET examinations, after repeated inflammatory challenges, with the aim to assess the immune response within the brain. Four previous human TSPO neuroimaging studies (Forsberg et al., 2017; Nettis et al., 2020; Sandiego et al., 2015; Woodcock et al., 2020), three in healthy volunteers and one in postoperative patients, examined the neuroinflammatory response after a single inflammatory stimulus. Our study differs on several topics from this previous work. First, inflammatory stimuli differed between studies in type and dosage, affecting the severity of the inflammatory insult. A recent study used interferon-α (IFN-α) as inflammatory stimulus (Nettis et al., 2020), which resulted in a very mild inflammatory response. Second, the timing of PET-scans ranged from 3 hours (Sandiego et al., 2015; Woodcock et al., 2020), 5 hours (present study), 24 hours (Nettis et al., 2020) and 3–4 days (Forsberg et al., 2017) after the inflammatory stimulus. Since *in vivo* data on the neuroinflammatory response during systemic inflammation are scarce, it is unknown to what extent timing of the scans affected the results. Our study made use of ^{18}F-DPA-714, which has the great advantage of having a longer half-life of ^{18}F, making it feasible to use in centres without an on-site cyclotron facility. With sufficient between-scan intervals, as in this study ($\geq$24 hours), there is no risk of carry-over effects during repeat scanning.

This study has several limitations. First, we only studied healthy young males. Biological characteristics such as age, sex, and body mass index (BMI) contribute significantly to TSPO binding estimates (Tuisku et al., 2019) and may therefore be confounders in clinical studies. Second, the statistical power of the study was affected by its limited size and missing scans, especially for the final post-LPS scan. Furthermore, the relatively small sample size likely resulted in overinflated correlation coefficients for the relationship between endotoxemia-induced clinical and inflammatory parameters and changes in binding potential, which should therefore be interpreted with caution. Since these longitudinal PET studies with human endotoxemia in healthy volunteers are quite invasive, challenging to conduct, as well as expensive, we could not replace subjects to increase the study power. Replication of our findings in another (larger) cohort is warranted. Fortunately, we found no case-mix differences and interindividual differences were small. Third, with this dataset we could not rule out inflammation-induced changes in ^{18}F-DPA-714 metabolism. However since the measured ^{18}F-DPA-714 metabolism post-LPS in our study was similar to previously published results in healthy volunteers without systemic inflammation (Arlicot et al., 2012), we made the assumption that the radiotracer metabolism did not change after an inflammatory stimulus. Moreover it should be mentioned that dynamic PET neuroimaging is designed with the assumption that the BBB remains intact. With increased BBB permeability, radiotracer metabolites that cannot bind to TSPO could cross the BBB and complicate the analysis. Inflammation is a well-established cause of BBB disruption, but since it has been shown that the BBB is relatively resistant to LPS-induced disruption (Banks et al., 2015), and we observed no change in the kinetic influx parameter after LPS administration, we expect the impact on our results negligible. Finally, TSPO expression is not specific to microglia and astrocytes and the measured PET signal can be driven by other factors such as recruitment of peripheral monocytes into the brain tissue, adherence of circulating leukocytes to the vascular epithelium, and expression of TSPO in neurons and vascular endothelial cells. Although we tried to correct for the endothelial component using the 2TCM-K1 model (Rizzo et al., 2014), this did not result in reliable ^{18}F-DPA-714 binding estimates.

Strengths of this study include that this is a human study with a longitudinal set-up and repeated strong LPS challenges, resulting in a wide range of inflammatory activation enabling us to detect strong correlations between the systemic and cerebral immune responses. In addition, we have not only shown neuroinflammatory responses following endotoxemia, but also revealed increases in TSPO on a transcriptional and functional level in peripheral blood cells, which are more easily accessible than tissue-resident immune cells. Our study includes extensive characterization of the systemic immune response. Finally, our setup presents a human experimental model that can be used to study cerebral immunotolerance in a very standardized, controlled experimental set-up.

In conclusion, we demonstrated a profound increase in cerebral immune activity after a first inflammatory stimulus with LPS, which was most pronounced in cortical brain regions. While systemic endotoxin

tolerance following the second inflammatory stimulus occurred, immune activity within the cerebral compartment was not attenuated but reduced. This may suggest cerebral reprogramming towards a more anti-inflammatory phenotype in humans, which may serve as a neuroprotective mechanism. Future studies are warranted to assess whether the presence or absence of differentiation towards an immunotolerant state is related to longer-term cerebral dysfunction in patients that suffered from systemic inflammation.

Declaration of Competing Interest

The authors declare that they have no known competing financial interests or personal relationships that could have appeared to influence the work reported in this paper.

Acknowledgments

The authors are grateful for the help of our colleagues at the section of Nuclear Medicine, especially Peter Laverman, Desirée Bos, Jurrian Butter, Peter Kok, Maichel van Riel, Natascha Verhoeven, Daphne Lobeek, Michel de Groot, Judith Thijssen, and Marijke Hogenkamp. In addition we wish to thank Jelle Gerretsen for his work in the laboratory and Christopher Geven, Hidde Heesakkers and Jelle Nijs for their help during the endotoxemia experiments. Special thanks to Ewald Bronkhorst (biostatistician) for his contribution to the statistical analyses.

Dr. W.F. Abdo and this study were supported by a research grant from the Netherlands Organization for Health Research and Development (ZonMW Clinical Fellowship Grant 90715610). This funding agency had no role in the concept, design, or writing of this study.

Appendix A. Supplementary data

Supplementary data to this article can be found online at https://doi.org/10.1016/j.bbi.2021.04.004.

References

Arlicot, N., Vercouillie, J., Ribeiro, M.J., Tauber, C., Venel, Y., Baulieu, J.L., Maia, S., Corcia, P., Stabin, M.G., Reynolds, A., Kassiou, M., Guilloteau, D., 2012. Initial evaluation in healthy humans of [18F]DPA-714, a potential PET biomarker for neuroinflammation. Nucl. Med. Biol. 39, 570–578.

Banks, W.A., Gray, A.M., Erickson, M.A., Salameh, T.S., Damodarasamy, M., Sheibani, N., Meabon, J.S., Wing, E.E., Morofuji, Y., Cook, D.G., Reed, M.J., 2015. Lipopolysaccharide-induced blood-brain barrier disruption: roles of cyclooxygenase, oxidative stress, neuroinflammation, and elements of the neurovascular unit. J. Neuroinflammation 12, 223.

Beckers, L., Ory, D., Geric, I., Declercq, L., Koole, M., Kassiou, M., Bormans, G., Baes, M., 2017. Increased Expression of Translocator Protein (TSPO) Marks Pro-inflammatory Microglia but Does Not Predict Neurodegeneration. Molecular imaging and biology : MIB : the official publication of the Academy of Molecular Imaging.

Boche, D., Cunningham, C., Docagne, F., Scott, H., Perry, V.H., 2006. TGFbeta1 regulates the inflammatory response during chronic neurodegeneration. Neurobiol. Dis. 22, 638–650.

Brites, D., Fernandes, A., 2015. Neuroinflammation and Depression: Microglia Activation, Extracellular Microvesicles and microRNA Dysregulation. Front. Cell. Neurosci. 9, 476.

Combrinck, M.I., Perry, V.H., Cunningham, C., 2002. Peripheral infection evokes exaggerated sickness behaviour in pre-clinical murine prion disease. Neuroscience 112, 7–11.

Cunningham, C., Campion, S., Lunnon, K., Murray, C.L., Woods, J.F., Deacon, R.M., Rawlins, J.N., Perry, V.H., 2009. Systemic inflammation induces acute behavioral and cognitive changes and accelerates neurodegenerative disease. Biol. Psychiatry 65, 304–312.

Cunningham, C., Wilcockson, D.C., Campion, S., Lunnon, K., Perry, V.H., 2005. Central and systemic endotoxin challenges exacerbate the local inflammatory response and increase neuronal death during chronic neurodegeneration. J. Neurosci. 25, 9275–9284.

Ehlenbach, W.J., Hough, C.L., Crane, P.K., Haneuse, S.J.P.A., Carson, S.S., Curtis, J.R., Larson, E.B., 2010. Association Between Acute Care and Critical Illness Hospitalization and Cognitive Function in Older Adults. JAMA 303, 763–770.

Forsberg, A., Cervenka, S., Jonsson Fagerlund, M., Rasmussen, L.S., Zetterberg, H., Erlandsson Harris, H., Stridh, P., Christensson, E., Granstrom, A., Schening, A., Dymmel, K., Knave, N., Terrando, N., Maze, M., Borg, J., Varrone, A., Halldin, C., Blennow, K., Farde, L., Eriksson, L.I., 2017. The immune response of the human brain to abdominal surgery. Ann. Neurol.

Godbout, J.P., Chen, J., Abraham, J., Richwine, A.F., Berg, B.M., Kelley, K.W., Johnson, R.W., 2005. Exaggerated neuroinflammation and sickness behavior in aged mice after activation of the peripheral innate immune system. FASEB J. 19, 1329–1331.

Golla, S.S., Boellaard, R., Oikonen, V., Hoffmann, A., van Berckel, B.N., Windhorst, A.D., Virta, J., Haaparanta-Solin, M., Luoto, P., Savisto, N., Solin, O., Valencia, R., Thiele, A., Eriksson, J., Schuit, R.C., Lammertsma, A.A., Rinne, J.O., 2015. Quantification of [18F]DPA-714 binding in the human brain: initial studies in healthy controls and Alzheimer's disease patients. J. Cereb. Blood Flow Metab. 35, 766–772.

Heneka, M.T., Carson, M.J., El Khoury, J., Landreth, G.E., Brosseron, F., Feinstein, D.L., Jacobs, A.H., Wyss-Coray, T., Vitorica, J., Ransohoff, R.M., Herrup, K., Frautschy, S. A., Finsen, B., Brown, G.C., Verkhratsky, A., Yamanaka, K., Koistinaho, J., Latz, E., Halle, A., Petzold, G.C., Town, T., Morgan, D., Shinohara, M.L., Perry, V.H., Holmes, C., Bazan, N.G., Brooks, D.J., Hunot, S., Joseph, B., Deigendesch, N., Garaschuk, O., Boddeke, E., Dinarello, C.A., Breitner, J.C., Cole, G.M., Golenbock, D. T., Kummer, M.P., 2015. Neuroinflammation in Alzheimer's disease. Lancet Neurol. 14, 388–405.

Honarmand, K., Lalli, R.S., Priestap, F., Chen, J.L., McIntyre, C.W., Owen, A.M., Slessarev, M., 2020. Natural History of Cognitive Impairment in Critical Illness Survivors. A Systematic Review. Am. J. Respir. Crit. Care Med. 202, 193–201.

Hughes, M.M., Field, R.H., Perry, V.H., Murray, C.L., Cunningham, C., 2010. Microglia in the degenerating brain are capable of phagocytosis of beads and of apoptotic cells, but do not efficiently remove PrPSc, even upon LPS stimulation. Glia 58, 2017–2030.

Innis, R.B., Cunningham, V.J., Delforge, J., Fujita, M., Gjedde, A., Gunn, R.N., Holden, J., Houle, S., Huang, S.C., Ichise, M., Iida, H., Ito, H., Kimura, Y., Koeppe, R.A., Knudsen, G.M., Knuuti, J., Lammertsma, A.A., Laruelle, M., Logan, J., Maguire, R.P., Mintun, M.A., Morris, E.D., Parsey, R., Price, J.C., Slifstein, M., Sossi, V., Suhara, T., Votaw, J.R., Wong, D.F., Carson, R.E., 2007. Consensus nomenclature for in vivo imaging of reversibly binding radioligands. J. Cereb. Blood Flow Metab. 27, 1533–1539.

Kettenmann, H., Hanisch, U.K., Noda, M., Verkhratsky, A., 2011. Physiology of microglia. Physiol. Rev. 91, 461–553.

Kurtz, J., 2005. Specific memory within innate immune systems. Trends Immunol. 26, 186–192.

Lavisse, S., Guillermier, M., Hérard, A.S., Petit, F., Delahaye, M., Van Camp, N., Ben Haim, L., Lebon, V., Remy, P., Dollé, F., Delzescaux, T., Bonvento, G., Hantraye, P., Escartin, C., 2012. Reactive astrocytes overexpress TSPO and are detected by TSPO positron emission tomography imaging. J. Neurosci. 32, 10809–10818.

Leentjens, J., Kox, M., Koch, R.M., Preijers, F., Joosten, L.A., van der Hoeven, J.G., Netea, M.G., Pickkers, P., 2012. Reversal of immunoparalysis in humans in vivo: a double-blind, placebo-controlled, randomized pilot study. Am. J. Respir. Crit. Care Med. 186, 838–845.

Leijte, G.P., Kiers, D., van der Heijden, W., Jansen, A., Gerretsen, J., Boerrigter, V., Netea, M.G., Kox, M., Pickkers, P., 2018. Treatment With Acetylsalicylic Acid Reverses Endotoxin Tolerance in Humans In Vivo: A Randomized Placebo-Controlled Study. Crit. Care Med.

Lopez-Rodriguez, A.B., Hennessy, E., Murray, C., Lewis, A., Barra, N.d., Fagan, S., Rooney, M., Nazmi, A., Cunningham, C., 2018. Microglial and Astrocyte priming in the APP/PS1 model of Alzheimer's Disease: increased vulnerability to acute inflammation and cognitive deficits. bioRxiv, 344218.

Medzhitov, R., Janeway Jr., C., 2000. Innate immune recognition: mechanisms and pathways. Immunol. Rev. 173, 89–97.

Mintun, M.A., Raichle, M.E., Kilbourn, M.R., Wooten, G.F., Welch, M.J., 1984. A quantitative model for the in vivo assessment of drug binding sites with positron emission tomography. Ann. Neurol. 15, 217–227.

Moller, J.T., Cluitmans, P., Rasmussen, L.S., Houx, P., Rasmussen, H., Canet, J., Rabbitt, P., Jolles, J., Larsen, K., Hanning, C.D., Langeron, O., Johnson, T., Lauven, P.M., Kristensen, P.A., Biedler, A., van Beem, H., Fraidakis, O., Silverstein, J. H., Beneken, J.E.W., Gravenstein, J.S., 1998. Long-term postoperative cognitive dysfunction in the elderly: ISPOCD1 study. The Lancet 351, 857–861.

Mondelli, V., Vernon, A.C., Turkheimer, F., Dazzan, P., Pariante, C.M., 2017. Brain microglia in psychiatric disorders. Lancet Psychiatry 4, 563–572.

Monk, T.G., Weldon, B.C., Garvan, C.W., Dede, D.E., van der Aa, M.T., Heilman, K.M., Gravenstein, J.S., 2008. Predictors of cognitive dysfunction after major noncardiac surgery. Anesthesiology 108, 18–30.

Netea, M.G., Joosten, L.A., Latz, E., Mills, K.H., Natoli, G., Stunnenberg, H.G., O'Neill, L. A., Xavier, R.J., 2016. Trained immunity: A program of innate immune memory in health and disease. Science 352, aaf1098.

Netea, M.G., Quintin, J., van der Meer, J.W., 2011. Trained immunity: a memory for innate host defense. Cell Host Microbe 9, 355–361.

Nettis, M.A., Veronese, M., Nikkheslat, N., Mariani, N., Lombardo, G., Sforzini, L., Enache, D., Harrison, N.A., Turkheimer, F.E., Mondelli, V., Pariante, C.M., 2020. PET imaging shows no changes in TSPO brain density after IFN-alpha immune challenge in healthy human volunteers. Transl. Psychiatry 10, 89.

Palin, K., Cunningham, C., Forse, P., Perry, V.H., Platt, N., 2008. Systemic inflammation switches the inflammatory cytokine profile in CNS Wallerian degeneration. Neurobiol. Disease 30, 19–29.

Pandharipande, P.P., Girard, T.D., Jackson, J.C., Morandi, A., Thompson, J.L., Pun, B.T., Brummel, N.E., Hughes, C.G., Vasilevskis, E.E., Shintani, A.K., Moons, K.G., Geevarghese, S.K., Canonico, A., Hopkins, R.O., Bernard, G.R., Dittus, R.S., Ely, E.W., 2013. Long-Term Cognitive Impairment after Critical Illness. N. Engl. J. Med. 369, 1306–1316.

Pannell, M., Economopoulos, V., Wilson, T.C., Kersemans, V., Isenegger, P.G., Larkin, J. R., Smart, S., Gilchrist, S., Gouverneur, V., Sibson, N.R., 2020. Imaging of

translocator protein upregulation is selective for pro-inflammatory polarized astrocytes and microglia. Glia 68, 280–297.
Perry, V.H., Cunningham, C., Holmes, C., 2007. Systemic infections and inflammation affect chronic neurodegeneration. Nat. Rev. Immunol. 7, 161–167.
Peyronneau, M.A., Saba, W., Goutal, S., Damont, A., Dolle, F., Kassiou, M., Bottlaender, M., Valette, H., 2013. Metabolism and quantification of [(18)F]DPA-714, a new TSPO positron emission tomography radioligand. Drug Metab. Dispos. 41, 122–131.
Philips, T., Robberecht, W., 2011. Neuroinflammation in amyotrophic lateral sclerosis: role of glial activation in motor neuron disease. Lancet Neurol. 10, 253–263.
Raj, D.D.A., Jaarsma, D., Holtman, I.R., Olah, M., Ferreira, F.M., Schaafsma, W., Brouwer, N., Meijer, M.M., de Waard, M.C., van der Pluijm, I., Brandt, R., Kreft, K.L., Laman, J.D., de Haan, G., Biber, K.P.H., Hoeijmakers, J.H.J., Eggen, B.J.L., Boddeke, H.W.G.M., 2014. Priming of microglia in a DNA-repair deficient model of accelerated aging. Neurobiol. Aging 35, 2147–2160.
Rakic, S., Hung, Y.M.A., Smith, M., So, D., Tayler, H.M., Varney, W., Wild, J., Harris, S., Holmes, C., Love, S., Stewart, W., Nicoll, J.A.R., Boche, D., 2018. Systemic infection modifies the neuroinflammatory response in late stage Alzheimer's disease. Acta Neuropathol Commun 6, 88.
Ramaglia, V., Hughes, T.R., Donev, R.M., Ruseva, M.M., Wu, X., Huitinga, I., Baas, F., Neal, J.W., Morgan, B.P., 2012. C3-dependent mechanism of microglial priming relevant to multiple sclerosis. Proc. Natl. Acad. Sci. 109, 965–970.
Rinaldi, M., Thomas, L., Mathieu, P., Carabias, P., Troncoso, M.F., Pasquini, J.M., Rabinovich, G.A., Pasquini, L.A., 2016. Galectin-1 circumvents lysolecithin-induced demyelination through the modulation of microglial polarization/phagocytosis and oligodendroglial differentiation. Neurobiology of disease 96, 127–143.
Rizzo, G., Veronese, M., Tonietto, M., Zanotti-Fregonara, P., Turkheimer, F.E., Bertoldo, A., 2014. Kinetic modeling without accounting for the vascular component impairs the quantification of [(11)C]PBR28 brain PET data. J. Cereb. Blood Flow Metab. 34, 1060–1069.
Rupprecht, R., Papadopoulos, V., Rammes, G., Baghai, T.C., Fan, J., Akula, N., Groyer, G., Adams, D., Schumacher, M., 2010. Translocator protein (18 kDa) (TSPO) as a therapeutic target for neurological and psychiatric disorders. Nat Rev Drug Discov 9, 971–988.
Sandiego, C.M., Gallezot, J.D., Pittman, B., Nabulsi, N., Lim, K., Lin, S.F., Matuskey, D., Lee, J.Y., O'Connor, K.C., Huang, Y., Carson, R.E., Hannestad, J., Cosgrove, K.P., 2015. Imaging robust microglial activation after lipopolysaccharide administration in humans with PET. PNAS 112, 12468–12473.
Schaafsma, W., Zhang, X., van Zomeren, K.C., Jacobs, S., Georgieva, P.B., Wolf, S.A., Kettenmann, H., Janova, H., Saiepour, N., Hanisch, U.K., Meerlo, P., van den Elsen, P.J., Brouwer, N., Boddeke, H.W.G.M., Eggen, B.J.L., 2015. Long-lasting pro-inflammatory suppression of microglia by LPS-preconditioning is mediated by RelB-dependent epigenetic silencing. Brain Behav. Immun. 48, 205–221.
Schedlowski, M., Engler, H., Grigoleit, J.S., 2014. Endotoxin-induced experimental systemic inflammation in humans: a model to disentangle immune-to-brain communication. Brain Behav. Immun. 35, 1–8.
Shah, F.A., Pike, F., Alvarez, K., Angus, D., Newman, A.B., Lopez, O., Tate, J., Kapur, V., Wilsdon, A., Krishnan, J.A., Hansel, N., Au, D., Avdalovic, M., Fan, V.S., Barr, R.G., Yende, S., 2013. Bidirectional relationship between cognitive function and pneumonia. Am. J. Respir. Crit. Care Med. 188, 586–592.
Song, G.J., Suk, K., 2017. Pharmacological Modulation of Functional Phenotypes of Microglia in Neurodegenerative Diseases. Frontiers in Aging Neuroscience 9.
Thackray, A.M., McKenzie, A.N., Klein, M.A., Lauder, A., Bujdoso, R., 2004. Accelerated Prion Disease in the Absence of Interleukin-10. J. Virol. 78, 13697.
Tuisku, J., Plaven-Sigray, P., Gaiser, E.C., Airas, L., Al-Abdulrasul, H., Bruck, A., Carson, R.E., Chen, M.K., Cosgrove, K.P., Ekblad, L., Esterlis, I., Farde, L., Forsberg, A., Halldin, C., Helin, S., Kosek, E., Lekander, M., Lindgren, N., Marjamaki, P., Rissanen, E., Sucksdorff, M., Varrone, A., Collste, K., Gallezot, J.D., Hillmer, A., Huang, Y., Hoglund, C.O., Johansson, J., Jucaite, A., Lampa, J., Nabulsi, N., Pittman, B., Sandiego, C.M., Stenkrona, P., Rinne, J., Matuskey, D., Cervenka, S., 2019. Effects of age, BMI and sex on the glial cell marker TSPO - a multicentre [(11)C]PBR28 HRRT PET study. Eur. J. Nucl. Med. Mol. Imaging 46, 2329–2338.
van Lier, D., Geven, C., Leijte, G.P., Pickkers, P., 2019. Experimental human endotoxemia as a model of systemic inflammation. Biochimie 159, 99–106.
Vivekanantham, S., Shah, S., Dewji, R., Dewji, A., Khatri, C., Ologunde, R., 2015. Neuroinflammation in Parkinson's disease: role in neurodegeneration and tissue repair. Int. J. Neurosci. 125, 717–725.
Wendeln, A.C., Degenhardt, K., Kaurani, L., Gertig, M., Ulas, T., Jain, G., Wagner, J., Häsler, L.M., Wild, K., Skodras, A., Blank, T., Staszewski, O., Datta, M., Centeno, T. P., Capece, V., Islam, M.R., Kerimoglu, C., Staufenbiel, M., Schultze, J.L., Beyer, M., Prinz, M., Jucker, M., Fischer, A., Neher, J.J., 2018. Innate immune memory in the brain shapes neurological disease hallmarks. Nature 556, 332–338.
Wolters, A.E., Slooter, A.J., van der Kooi, A.W., van Dijk, D., 2013. Cognitive impairment after intensive care unit admission: a systematic review. Intensive Care Med. 39, 376–386.
Woodcock, E.A., Hillmer, A.T., Sandiego, C.M., Maruff, P., Carson, R.E., Cosgrove, K.P., Pietrzak, R.H., 2020. Acute neuroimmune stimulation impairs verbal memory in adults: A PET brain imaging study. Brain Behav. Immun.
Yin, Z., Raj, D., Saiepour, N., Van Dam, D., Brouwer, N., Holtman, I.R., Eggen, B.J.L., Möller, T., Tamm, J.A., Abdourahman, A., Hol, E.M., Kamphuis, W., Bayer, T.A., De Deyn, P.P., Boddeke, E., 2017. Immune hyperreactivity of Aβ plaque-associated microglia in Alzheimer's disease. Neurobiol. Aging 55, 115–122.